THE JOURNAL OF BIOLOGICAL CHEMISTRY VOL. 281, NO. 46, pp. 35413–35424, November 17, 2006

Interactions between TonB from *Escherichia coli* and the Periplasmic Protein FhuD*

Received for publication, August 9, 2006 Published, JBC Papers in Press, August 23, 2006, DOI 10.1074/jbc.M607611200

David M. Carter[‡1], Isabelle R. Miousse[‡2], Jean-Nicolas Gagnon[‡3], Éric Martinez[‡4], Abigail Clements[‡5], Jongchan Lee[‡], Mark A. Hancock[§], Hubert Gagnon[‡], Peter D. Pawelek[‡6], and James W. Coulton[‡7]

From the [‡]Department of Microbiology and Immunology, and [§]Sheldon Biotechnology Centre, McGill University, Montreal, Quebec H3A 2B4, Canada

For uptake of ferrichrome into bacterial cells, FhuA, a TonB-dependent outer membrane receptor of *Escherichia coli*, is required. The periplasmic protein FhuD binds and transfers ferrichrome to the cytoplasmic membrane-associated permease FhuB/C. We exploited phage display to map protein-protein interactions in the *E. coli* cell envelope that contribute to ferrichrome transport. By panning random phage libraries against TonB and against FhuD, we identified interaction surfaces on each of these two proteins. Their interactions were detected *in vitro* by dynamic light scattering and indicated a 1:1 TonB-FhuD complex. FhuD residue Thr-181, located within the siderophore-binding site and mapping to a predicted TonB-interaction surface, was mutated to cysteine. FhuD T181C was reacted with two thiol-specific fluorescent probes; addition of the siderophore ferricrocin quenched fluorescence emissions of these conjugates. Similarly, quenching of fluorescence from both probes confirmed binding of TonB and established an apparent K_D of ~300 nM. Prior saturation of the siderophore-binding site of FhuD with ferricrocin did not alter affinity of TonB for FhuD. Binding, further characterized with surface plasmon resonance, indicated a higher affinity complex with K_D values in the low nanomolar range. Addition of FhuD to a preformed TonB-FhuA complex resulted in formation of a ternary complex. These observations led us to propose a novel mechanism in which TonB acts as a scaffold, directing FhuD to regions within the periplasm where it is poised to accept and deliver siderophore.

Iron, an essential nutrient for almost all bacterial species, is required for metabolic processes, including electron transfer, oxygen activation, and biosynthesis of amino acids and nucleosides (1). However, Fe^{3+} is scarce in the extracellular environment. Gram-negative bacteria have evolved transport processes that utilize siderophores to scavenge extracellular Fe^{3+} by high affinity chelation. Different siderophore receptors are expressed at the bacterial outer membrane (OM),[8] each with specificity for a particular metal-chelated siderophore. Transport of receptor-bound siderophores into the periplasm requires contribution of energy provided by the TonB-ExbB-ExbD complex that is anchored in the cytoplasmic membrane (CM). TonB spans the periplasm to make contacts with cognate OM receptors. By harnessing energy produced from the proton motive force, TonB may propagate conformational changes to OM siderophore receptors, resulting in release of siderophore into the periplasm.

The ferrichrome transport system consists of four proteins (FhuA, FhuB, FhuC, and FhuD) expressed by Gram-negative bacteria. The FhuA protein consists of two domains as follows: an N-terminal globular cork domain is enclosed by a 22-stranded C-terminal β-barrel domain (2, 3). Connections between β-strands in the barrel domain are such that long loops participating in ferrichrome binding are exposed to the extracellular environment; short turns are exposed to the periplasm. Uptake of ferrichrome is a TonB-dependent process, mediated by contacts between TonB and the OM receptor FhuA. TonB is elongated and has three domains as follows: an N-terminal domain anchored in the CM, an intermediate domain containing Pro-Glu and Pro-Lys repeats, and a globular C-terminal domain with a central β-sheet and two α-helices. To date, structural data are only available for the C-terminal domain (4–6). We recently solved the crystal structure of the 1:1 TonB-FhuA complex (7). The C-terminal domain of TonB makes extensive contacts with the N-terminal consensus Ton box of FhuA, as well as residues Ala-26 and Glu-56 of the cork domain and with periplasmic turns 8 and 10. These contacts orient TonB

* This work was supported in part by Operating Grant MOP-62774 (to J. W. C.) from the Canadian Institutes of Health Research. The costs of publication of this article were defrayed in part by the payment of page charges. This article must therefore be hereby marked "*advertisement*" in accordance with 18 U.S.C. Section 1734 solely to indicate this fact.

[1] Recipient of the McGill Graduate Studies Fellowship and an F. C. Harrison Fellowship.
[2] Recipient of a Natural Sciences and Engineering Research Council (Canada) Undergraduate Student Research Award.
[3] Recipient of a postgraduate scholarship.
[4] Trainee from the École Supérieure de Biotechnologie, Strasbourg, France. Present address: Dept. of Life Science, Imperial College, London, UK.
[5] Recipient of a traveling award for research training from the National Health and Medical Research Council (Australia). Present address: Dept. of Microbiology and Immunology, The University of Melbourne, Parkville, Australia.
[6] Present address: Dept. of Chemistry and Biochemistry, Concordia University, Montreal, Quebec H4B 1R6, Canada.
[7] To whom correspondence should be addressed: Dept. of Microbiology and Immunology, McGill University, 3775 University St., Montreal, Quebec H3A 2B4, Canada. Tel.: 514-398-3929; Fax: 514-398-7052; E-mail: james.coulton@mcgill.ca.

[8] The abbreviations used are: OM, outer membrane; CM, cytoplasmic membrane; Fcn, ferricrocin; DLS, dynamic light scattering; SPR, surface plasmon resonance; r.m.s.d., root mean square deviation; BSA, bovine serum albumin; MBP, maltose-binding protein; AEDANS, 5-((((2-iodoacetyl)amino)ethyl)amino)naphthaline-1-sulfonic acid; RU, response units; MDCC, 7-diethylamino-3-((((2-maleimidyl)ethyl)amino)carbonyl)coumarin; PDB, Protein Data Bank; DNS, discrete noninteracting species; *Rh*, hydrodynamic radius.

such that it may mediate conformational disruption of the internal cork domain of FhuA, allowing for passage of siderophore into the periplasm.

Although recent structural and biophysical data have clarified initial steps of the siderophore transport cycle involving TonB-receptor interactions, little is known about the fate of the siderophore once transported into the periplasm. Specifically, the molecular mechanisms of siderophore transport from periplasm to cytoplasm are largely uncharacterized. FhuD in the periplasm binds the hydroxamate siderophores ferrichrome, coprogen, and aerobactin (8). Loss of FhuD function *in vivo* prevented growth of *Escherichia coli* under iron-limiting conditions when ferrichrome, coprogen, or aerobactin were used as the sole iron source, suggesting that FhuD is a necessary component of the hydroxamate siderophore transport system (8). FhuD was reported to interact with regions of the CM-embedded permease FhuB. Interactions between FhuD and FhuB have been demonstrated by cross-linking studies, protease protection assays (9), and enzyme-linked immunosorbent assay (10). Interaction of FhuB with FhuD is apparently independent of siderophore binding by FhuD (9). Taken together, these results suggest that FhuD functions as a carrier protein; ferrichrome released from the OM receptor is delivered by FhuD to the permease. The integral membrane protein FhuB then translocates the siderophore into the cytoplasm mediated by ATP hydrolysis of FhuC (11).

The crystal structure of FhuD in complex with gallichrome, a ferrichrome analogue, has been reported (12), as well as structures of FhuD in complex with albomycin, coprogen, and Desferal® (13). The fold of this 32-kDa protein is bilobal; globular N- and C-terminal domains are connected by a long α-helix that confers rigidity to the protein. The siderophore-binding site residing in a shallow cleft between the two lobes is hydrophobic, having predominantly aromatic residues. Siderophore binds to FhuD through both hydrophobic and hydrophilic interactions. Methylene carbon atoms in the siderophore form hydrophobic interactions with numerous aromatic FhuD residues in the binding cleft. Hydrogen bonds are formed between hydroxamate groups of the siderophore and FhuD residues Arg-84 and Tyr-106. A hydrogen bond with the siderophore is also formed with FhuD residues Asn-215 and Ser-219 through an intermediate water molecule. The overall fold of FhuD is similar to that of BtuF (14, 15), the periplasmic cobalamin-binding protein of *E. coli*. Periplasmic metal-binding proteins TroA (16) and PsaA (17) are also structurally related to FhuD. These proteins share a fold distinct from those of classical periplasmic proteins such as maltose-binding protein (18). However, unlike maltose-binding protein, FhuD does not exhibit gross conformational rearrangements upon ligand binding. The linker connecting the N-terminal and C-terminal domains in FhuD is a kinked α-helix that crosses these domains only once. The structure of FhuD and the hydrophobicity of the siderophore-binding site suggest that large scale opening and closing of the binding site does not occur upon siderophore binding and release (18). Molecular dynamics simulations also suggest that FhuD is conformationally rigid but that subtle conformational differences in the C-terminal domain between the apo- and holo-forms may be sufficient for discrimination by FhuB (19).

What molecular events result in capture of ferrichrome by FhuD following its TonB-dependent release from FhuA? Given the apparent weak affinity (1 μM) of ferrichrome for FhuD (9), binding is unlikely to be a diffusion-governed process. Efficiency of siderophore capture would be enhanced by positioning a binding protein proximal to the lumen of the OM receptor. This organization would promote direct transfer of ferrichrome from FhuA to FhuD. Here we report the first biophysical evidence that TonB specifically interacts with FhuD. Discrete regions of protein-protein interactions on the surfaces of both FhuD and TonB were identified by phage display. Interactions were confirmed by dynamic light scattering, fluorescence spectroscopy, and surface plasmon resonance. Our results suggest that siderophore released from FhuA during the transport cycle is transferred to FhuD via a coordinated transfer mechanism mediated by TonB. Hence, TonB would act as a periplasm-spanning scaffold, directly connecting siderophore transport events between the OM and CM.

EXPERIMENTAL PROCEDURES

Bacterial Strains, Phage Libraries, and Media—Random peptide phage libraries Ph.D.-C7C and Ph.D.-12 were purchased from New England Biolabs; *E. coli* ER2738, also from New England Biolabs, was used for amplification and titration of phage M13 pools. *E. coli* ER2566 was used to express recombinant TonBs (20); *E. coli* BL21 (DE3) pLysS was used to express recombinant FhuDs. Plasmid pCMK01 expresses a hexahistidine-tagged TonB 32-239 (25 kDa; hereafter identified as TonB), and pWA01 expresses a hexahistidine-tagged TonB 32-239 with an engineered cysteine residue at its N terminus (hereafter identified as Cys-TonB) (21, 22). FhuD was expressed from pMR21 provided by W. Köster (VIDO, Saskatoon, Saskatchewan, Canada); the N terminus of FhuD containing the signal sequence was removed and replaced by a decahistidine tag (23) (32 kDa; hereafter identified as FhuD). Plasmid pMR21 was commercially mutated to cysteine at Thr-81 by Norclone Biotech Laboratories (London, Ontario, Canada); this protein is hereafter identified as FhuD T181C. Mutagenesis was confirmed by DNA sequencing at Sheldon Biotechnology Centre, McGill University (Montreal, Quebec, Canada). All bacteria were cultured in Luria Bertani (LB) broth containing antibiotics when necessary.

Chemicals and Reagents—5-Bromo-4-chloro-3-indolyl-β-D-galactopyranoside (X-gal) and isopropyl β-D-thiogalactopyranoside were purchased from BioVectra (Charlottetown, Prince Edward Island, Canada). Protein-grade Tween 20 was purchased from Calbiochem. Antibiotics were purchased from Sigma. Nickel-nitrilotriacetic acid resin used for protein purifications was purchased from Qiagen. The reducing agent tris-(2-carboxyethyl)phosphine and fluorescent dyes 5-((((2-iodoacetyl)amino)ethyl)amino)naphthaline-1-sulfonic acid (AEDANS) and 7-diethylamino-3-((((2-maleimidyl)ethyl)amino)carbonyl)coumarin (MDCC) were purchased from Invitrogen.

Protein Purification—TonB and Cys-TonB were purified as described previously (20). To purify overexpressed FhuD or FhuD T181C, cell pellets were suspended in 50 ml of buffer A containing 50 mM Tris, pH 8.2, 150 mM NaCl, and 5 mM imidazole plus one Complete mini EDTA-free protease inhibitor mixture tablet (Roche Applied Science); 0.16 mg/ml lysozyme and 16 μM phenylmethylsulfonyl fluoride were then added.

Cells were shaken at room temperature for 30 min, followed by addition of 0.04 mg/ml DNase, 0.04 mg/ml RNase, and an additional 16 μM phenylmethylsulfonyl fluoride. To lyse bacteria, cells were passed twice through an Emulsiflex-C5 (Avestin, Ottawa, Ontario, Canada). Cell lysate was centrifuged (27,000 × *g*, 4 °C) for 50 min and filtered through 0.45-μm syringe filters. Filtered cell extracts containing FhuD or FhuD T181C were applied to nickel-nitrilotriacetic acid resin equilibrated with buffer A. FhuDs were eluted with 50 mM Tris, pH 8.2, containing 125 mM imidazole, pooled, and applied to a POROS HQ 20 anion exchange column (Applied Biosystems). Bound proteins were washed with 50 mM Tris, pH 8.2, containing 125 mM imidazole, eluted with 160 mM NaCl, and applied inline to a POROS MC 20 column (Applied Biosystems). After extensive washing, proteins were eluted with 50 mM Tris, pH 8.2, and 120 mM imidazole and applied to a second POROS HQ 20 column, washed as described above, and eluted with 180 mM NaCl in 50 mM Tris, pH 8.2. Purified proteins were dialyzed in a 24,000 M_r cut-off dialysis membrane (SpectraPor) for 16 h at 4 °C in 100 mM Hepes, 150 mM NaCl, pH 7.4. Homogeneity of FhuDs was confirmed by SDS-PAGE and silver staining of 750 ng of total protein. Concentrations of protein were determined by either a Bradford or BCA assay using bovine serum albumin as standard.

Phage Display—Phage panning against TonB as target was described previously (24). Purified FhuD was diluted to 100 μg/ml in TBS (Tris-buffered saline: 50 mM Tris, pH 7.5, 150 mM NaCl), and 150 μl of protein was adsorbed to a polystyrene microtiter plate (Nunc Maxisorp). Plates coated with immobilized FhuD were incubated for 16 h at 4 °C followed by blocking (2 h at 37 °C) with TBS containing 5 mg/ml bovine serum albumin. The unselected phage library (New England Biolabs) was then added. Phage panning, clone isolation, DNA sequencing, and bioinformatic analyses were performed as described previously (24).

Dynamic Light Scattering—Light scattering was measured from purified TonB and FhuD dialyzed twice (18 h, 4 °C) in 100 mM Hepes, pH 7.4, containing 150 mM NaCl. Purified [Fhu switch-MBP] fusion protein (24) (containing FhuA residues ^{21}AWGPAAT^{27} fused to the N terminus of maltose-binding protein) and BSA were dialyzed against the same buffer and used in DLS measurements as positive and negative controls, respectively. TonB (4.0 μM) and FhuD (3.0 μM) were separately analyzed as discrete scattering species. Similarly, BSA (1.5 μM) and [Fhu switch-MBP] (2.5 μM) were analyzed separately. For a 1:1 molar ratio of TonB to FhuD, each protein at 1.7 μM was mixed prior to recording DLS readings. For 1:1 mixtures of TonB with BSA or with [Fhu switch-MBP], proteins were each at 1.0 μM. Protein mixtures were incubated for 30 min at room temperature prior to centrifugation and analysis. Data acquisition was performed in a 12-μl quartz cuvette at 20 °C using a temperature-controlled DynaPro E-50-830 dynamic light scattering instrument (Protein Solutions, Charlottesville, VA). The scattering signal was measured at a wavelength of 824.9 nm and an angle of 90°. Data were collected for 7000 s with a 10-s averaging time and replicated with two independent protein preparations. From the Dynamics version 6.3.18 software (Protein Solutions, Charlottesville, VA), data were filtered (base line <1.01 and sum of squares <500) before exporting to Sedfit version 9.3. Analyses of hydrodynamic radii (*Rh*) were performed using the continuous intensity distribution model (25) in Sedfit at a resolution of 100 for radii between 1 and 50 nm. Buffer densities and viscosities were set to 1.00442 and 0.01065, respectively, as determined by Sednterp version 1.08. All values of *Rh* from the Dynamics software exhibited less than 14% polydispersity, except for the TonB-FhuD mixture and [Fhu switch-MBP] (21 and 19%, respectively).

For Sedfit analyses of discrete noninteracting species (DNS), autocorrelation data sets were imported from the Dynamics software package and fit to a single species field autocorrelation function. Values of *s* for TonB were determined previously (20). Using analytical ultracentrifugation, we determined by sedimentation velocity experiments sedimentation coefficients for FhuD and the TonB-FhuD complex, 2.27 *s* and 3.5 *s*, respectively. From literature reports, *s* values for MBP (26) and BSA (27) were obtained. All were constrained in DNS analyses. Molecular mass values for discrete scattering species, either uncomplexed TonB, uncomplexed FhuD, or 1:1 heterocomplexes, were initially set to predicted values and then refined by nonlinear regression until r.m.s.d. errors were minimized. In addition to proteins TonB, FhuD, [Fhu switch-MBP], or complexes formed by these proteins, two scattering species were observed; the Dynamics program predicted these uncharacterized species to have hydrodynamic radii of ~1 and ~100 nm respectively. Hydrodynamic parameters for these species were factored into DLS analyses to optimize fits to the autocorrelation function.

Fluorescence Spectroscopy—The fluorescent dye AEDANS was conjugated to FhuD and FhuD T181C in a reaction buffer of 100 mM Hepes, pH 7.4, 150 mM NaCl. Following reduction of disulfide bonds with a 10-fold molar excess of tris-(2-carboxyethyl)phosphine, dye was added to a 10-fold molar excess. Conjugation proceeded in the dark with stirring for 4 h at room temperature. Reactions were quenched by addition of β-mercaptoethanol. Excess label was removed by exhaustive dialysis against four 1-liter changes of 100 mM Hepes, pH 7.4, containing 150 mM NaCl in the dark at 4 °C. After dialysis, free dye was present at picomolar concentrations. Conjugates were then centrifuged at 18,000 × *g* for 30 min at 4 °C. Labeled proteins were stored at 4 °C in the dark. Conjugation of FhuD T181C with the dye MDCC was performed as described above except that MDCC was dissolved in Me_2SO prior to its addition to protein. Efficiency of labeling (mol dye:mol protein) was calculated from absorption data using the following tabulated (Invitrogen) molar extinction coefficients: 5700 M^{-1} cm^{-1} at 336 nm for AEDANS and 50,000 M^{-1} cm^{-1} at 419 nm for MDCC and from protein concentrations as determined by protein assays.

Fluorescence data were collected with a Varian Cary Eclipse fluorescence spectrophotometer. Emission spectra were recorded at excitation and emission wavelengths of 280 and 340 nm, respectively, for intrinsic fluorescence measurements; at 336 and 490 nm, respectively, for AEDANS-labeled FhuD and FhuD T181C; and at 419 and 466 nm, respectively, for MDCC-labeled FhuD T181C. Excitation and emission slits were set between 2.5 and 5 nm and 5 and10 nm, respectively. Measurements were taken in triplicate at 20 °C. Data were corrected for changes in fluorescence intensity attributed to dilution of protein and the minimal fluorescence contributions of Fcn, TonB, and buffer (100 mM Hepes, pH 7.4, 150 mM NaCl).

TABLE 1
RELIC/MATCH identification of TonB affinity-selected Ph.D.-C7C peptides corresponding to FhuD sequences

Peptide[a]	Peptide match score[b]	Scoring window (residues)	Region	Alignment position[c]
PYGAALH	16	5	Loop 2	26
P**YGAAL**H	16	5	Loop 23	245
Y**GGATL**L	15	5	Loop 23	245
QP**AVANT**	13	5	Loop 2	28
SY**LNVMH**	13	5	Loop 23	249
TG**PLPN**R	13	4	Helix 2	43
N**PTPE**KR	13	4	Loop 8	78
KP**SSPP**F	12	4	Helix 2	40

[a] Residues contained in scoring window are shown in boldface type.
[b] Sum of pairwise comparisons of aligned residues within the scoring window.
[c] Position of first residue of the scoring window numbering from the N terminus of the mature protein.

TABLE 2
RELIC/MATCH identification of TonB affinity-selected Ph.D.-12 peptides corresponding to FhuD sequences

Peptide[a]	Peptide match score[b]	Scoring window (residues)	Region	Alignment position[c]
LL**ADTTHHR**PWT	17	7	Loop 2	30
HWKH**PWGAWDT**L	16	7	Loop 2	26
KVWSL**EPPGP**AA	15	5	Helix 2	41
YSP**PSPEP**PRIK	15	5	Loop 8	78
QD**RGILVEPP**RM	14	8	Helix 2	36
D**FDVSFLSA**RMR	14	8	Loop 23	244
K**LWELNPP**QVRT	14	7	Helix 2	37
SP**APTNNY**TYRL	14	6	Loop 2	30
TQP**LGLLP**SRHL	14	5	Loop 2	22
QTALI**TIHHSL**T	13	6	Loop 2	32
YGNSLPPRLGPP	13	5	Loop 23	245
LWA**KLWV**VPERA	12	5	Helix 2	36
SANLSWRESWPT	12	5	Loop 23	246

[a] Residues contained in scoring window are shown in boldface type.
[b] Sum of pairwise comparisons of aligned residues within the scoring window.
[c] Position of first residue of the scoring window numbering from the N terminus of the mature protein.

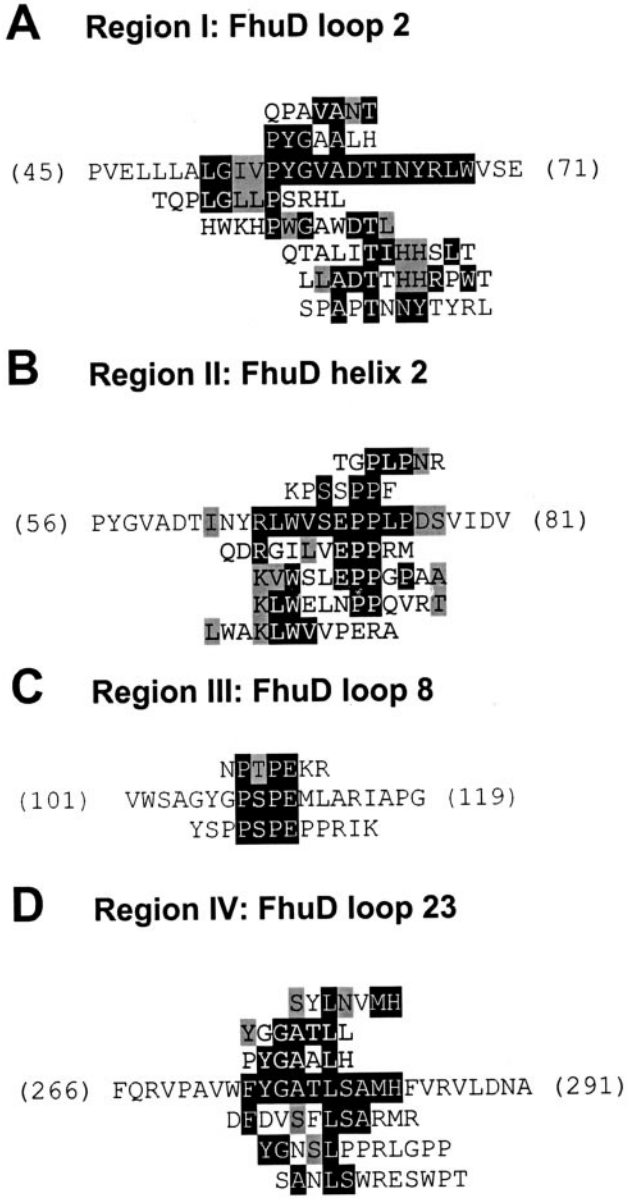

FIGURE 1. **Alignments of TonB affinity-selected peptides to FhuD as identified by RELIC/MATCH.** *A, region I,* FhuD loop 2; *B, region II,* FhuD helix 2; *C, region III,* FhuD loop 8; *D, region IV,* FhuD loop 23. Peptides from the Ph.D.-12 library are aligned below the FhuD sequence; peptides from the Ph.D.-C7C library are aligned above the FhuD sequence. See Tables 1 and 2 for peptide match scores and window sizes. Alignment positions are highlighted according to their pairwise alignment score: +4, *black background* and *white characters*; +1, *gray background* and *dark characters.*

Binding of Fcn to either FhuD (1.5 μM) or FhuD T181C (0.5 μM) was monitored by recording the fluorescence emission after additions of Fcn up to a 10-fold molar excess. For each data point, Fcn was added from a stock solution, and after 3 min of incubation, the change in fluorescence was recorded. Titrations of labeled conjugates with either Fcn or TonB were conducted in an identical manner. Fluorescence quenching was expressed as the percentage decrease in fluorescence upon ligand addition compared with the theoretical maximum whereby quenching would result in complete loss of fluorescence. Data were fit (Sigmaplot) to an equation describing a rectangular hyperbola using the single binding site model or to a sum of two hyperbolics using the model that describes two independent binding sites.

Surface Plasmon Resonance (SPR)—Binding interactions between TonB and FhuD or between Cys-TonB and FhuD were examined in real time using BIAcore 2000/3000 instrumentation with research grade CM4 sensor chips (BIAcore AB, Uppsala, Sweden). Experiments were performed in triplicate at 25 °C using filtered (0.2 μm) and degassed HBS-ET (50 mM Hepes, pH 7.4, 150 mM NaCl, 3 mM EDTA, 0.05% (v/v) Tween 20). 1-Ethyl-3-(3-dimethylaminopropyl)-carbodiimide, *N*-hydroxysuccinimide, and 2-(2-pyridinyldithio)ethaneamine were from BIAcore AB. Protein grade detergents (10% Tween 20, 10% Triton X-100, 30% Empigen) were from Calbiochem. All other chemicals were reagent grade quality.

For amine coupling, TonB was immobilized according to a standard BIAcore protocol. For ligand thiol-coupling, 20 μl of freshly mixed solution I (200 mM 1-ethyl-3-(3-dimethylaminopropyl)-carbodiimide and 50 mM *N*-hydroxysuccinimide in water) was injected (5 μl/min) over the sensor chip activating carboxymethyl groups to reactive esters. Reactive thiol groups were then introduced by a 30-μl injection of freshly prepared solution II (80 mM 2-(2-pyridinyldithio) ethaneamine in 0.1 M sodium borate, pH 8.5). Diluted Cys-TonB ligand (3 μg/ml in 10 mM sodium acetate, pH 4.5) was

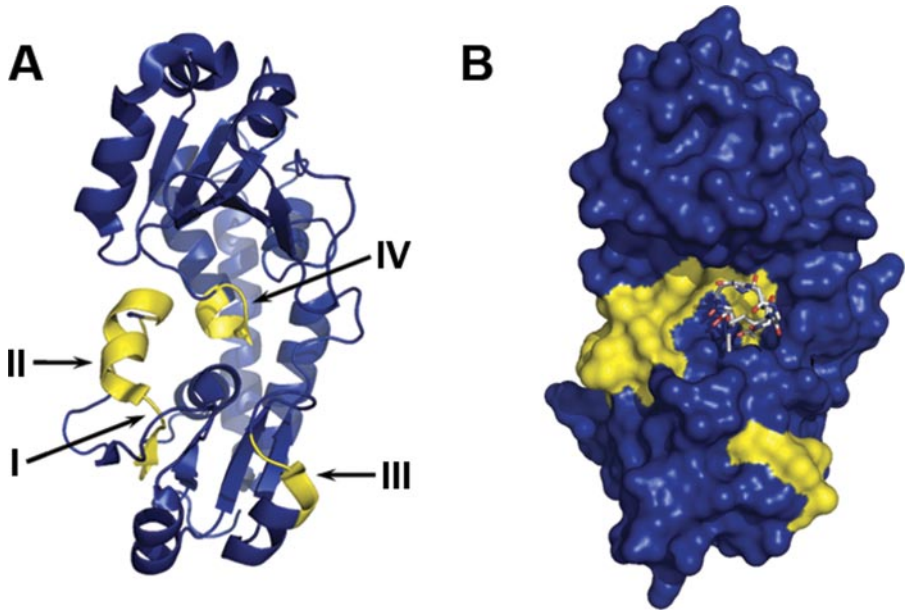

FIGURE 2. **TonB-binding regions identified by phage display mapped to FhuD (PDB code 1EFD).** *A,* ribbon representation of FhuD (*blue*) with predicted TonB-binding regions *shaded yellow*. Regions corresponding to RELIC/MATCH alignment clusters shown in Fig. 1 are indicated by roman numerals: *I,* loop 2; *II,* helix 2; *III,* loop 8; *IV,* loop 23. *B,* molecular surface representation of FhuD (*blue*) with predicted TonB-binding regions *shaded yellow*. The bound ligand gallichrome from the 1EFD structure is shown in stick representation and colored by atoms (carbon, *white*; nitrogen, *blue*; oxygen, *red*).

injected manually until ~120 RU were bound. Finally, three injections (20 μl) of freshly prepared solution III (50 mM L-cysteine in 0.1 M sodium formate, pH 4.3, containing 1 M NaCl) deactivated excess reactive groups and removed any nonspecifically bound ligand. Coupling efficiencies were typically ~50%. Reference surfaces were prepared in a similar manner without any ligand addition.

Immobilized TonB and Cys-TonB surfaces were washed overnight at 5 μl/min in running buffer. Prior to use, FhuD analyte was dialyzed against HBS-ET, and immobilized TonB or Cys-TonB surfaces were conditioned at 50 μl/min using regeneration scheme A as follows: two 25-μl injections each of (i) 0.05% (v/v) Empigen, 0.5 M NaCl, 50 mM EDTA, 10 mM NaOH in HBS-ET, (ii) 0.05% (v/v) Triton X-100, 0.5 M NaCl, 50 mM EDTA, 10 mM NaOH in HBS-ET, and (iii) HBS-ET. For kinetic experiments, FhuD (0.1–1 μM in the absence and presence of a 10-fold molar excess of Fcn) was injected at 50 μl/min (120 s association + 120 s dissociation) over amine-coupled TonB or thiol-coupled Cys-TonB. Surface performance and mass transfer tests confirmed that the ligand density and regeneration conditions were appropriate. All acquired data were double-referenced (28) and analyzed globally according to the simple 1:1 binding model ($A + B = AB$) or to the heterogeneous ligand model in the BIAevaluation 4.1 software (BIAcore AB). Kinetic estimates represent fits to the experimental data with χ^2 values below 1.

Multicomponent SPR analyses between FhuA, TonB, and FhuD were performed. Initially, amine-coupled TonB surfaces (250 RU) or thiol-coupled Cys-TonB surfaces (100 RU) were prepared. Then, either a TonB-FhuA or a TonB-FhuD binary complex was formed by injecting each analyte at 50 μl/min. By injecting FhuD over TonB-FhuA complexes or by injecting FhuA over TonB-FhuD complexes, ternary complex formation was assessed.

RESULTS

Identification of TonB-binding Sites on FhuD by Phage Display—Following affinity selection *versus* immobilized TonB (24), 135 unique disulfide-constrained peptides from the Ph.D.-C7C library and 105 unique linear peptides from the Ph.D.-12 library were analyzed. These phage-displayed peptides were scanned for their similarity to the primary sequence of FhuD using the receptor ligand contacts (RELIC) program RELIC/MATCH (29). Among these sequences, 8 from the Ph.D.-C7C library (Table 1) and 13 from the Ph.D.-12 library (Table 2) were found to share similarities with the primary sequence of FhuD. The Ph.D.-C7C and Ph.D.-12 sequences were observed (Fig. 1) to cluster at four discrete regions along FhuD as follows: loop 2 (region I), helix 2 (Region II), loop 8 (region III), and loop 23 (region IV). When these four regions were mapped (Fig. 2*A*) onto the surface of the three-dimensional structure of FhuD (PDB code 1EFD), they displayed a binding surface that overlaps the siderophore-binding site (Fig. 2*B*). Regions I, II, and IV comprise a continuous binding surface of ~17 × 17 Å that is formed at the base of the siderophore binding pocket. In addition to loop 23, region IV also includes residues from helix 13 near the C terminus of FhuD. Although the surface-exposed residues in region III could form a potential TonB-binding landscape with regions I, II, and IV, residues 81–88 in loop 3 preclude formation of such a continuum. No FhuD residues within this interval were identified by our phage display analysis, suggesting that loop 3 is not TonB-binding. If there was a continuous landscape of all four regions, it would require a displacement of loop 3 from FhuD to accommodate TonB binding. Recent molecular dynamics simulations on the FhuD structure (19) indicated that the C-terminal domain of FhuD has more overall mobility than the N-terminal domain. However, within the relatively static N-terminal domain, loop 3 was observed to be the most mobile region.

Identification of FhuD-binding Sites on TonB by Phage Display—Purified FhuD was immobilized and sequentially panned with the Ph.D.-C7C library and with the Ph.D.-12 library. Panning yielded 109 unique sequences from the Ph.D.-C7C library and 38 unique sequences from the Ph.D.-12 library. Of these sequences, 15 from the Ph.D.-C7C library (Table 3) and 10 from the Ph.D.-12 library (Table 4) were found by RELIC/MATCH to be similar to the primary sequence of TonB. When aligned to TonB, these sequences were observed (Fig. 3) to cluster at three discrete TonB regions as follows: an N-terminal domain (region I), an intermediate domain (region II),

TABLE 3
RELIC/MATCH identification of FhuD affinity-selected Ph.D.-C7C peptides corresponding to TonB sequences

Peptide[a]	Peptide match score[b]	Scoring window (residues)	Region	Alignment position[c]
PAPERPQ	16	6	N-terminal	39
H**ASPAHN**	15	6	Intermediate	121
VISAASQ	15	6	C-terminal	146
Q**SFPRQL**	14	6	C-terminal	149
NRPSSWL	14	5	Intermediate	119
TA**ENSSP**	13	5	Intermediate	124
KTSPAWI	13	5	Intermediate	127
MT**ARTTS**	13	5	Intermediate	129
I**SPAQ**SS	13	4	N-terminal	39
PA**VPAKA**	12	5	N-terminal	36
HLAPAAR	12	5	Intermediate	127
KALMRTS	12	5	C-terminal	153
KPL**FHNT**	12	4	Intermediate	122
HHW**APTR**	12	4	Intermediate	126
HNM**PAQ**T	12	3	N-terminal	38

[a] Residues contained in scoring window are shown in boldface type.
[b] Sum of pairwise comparisons of aligned residues within the scoring window.
[c] Position of first residue of the scoring window numbering from the N terminus of the mature protein.

TABLE 4
RELIC/MATCH identification of FhuD affinity-selected Ph.D.-12 peptides corresponding to TonB sequences

Peptide[a]	Peptide match score[b]	Scoring window (residues)	Region	Alignment position[c]
LHTPWH**LPAP**EI	16	4	N-terminal	32
KSLSRHDHIHHH	15	6	C-terminal	153
YHSPPH**TPPAPL**	14	6	Intermediate	122
SFVG**LVELP**QNL	14	5	N-terminal	31
VSRHQSWHPHDL	14	5	C-terminal	155
KTLTL**PLSNTS**K	13	6	Intermediate	119
KIMRMP**RLMTRN**	13	6	C-terminal	147
LHFPLDY**PQALG**	13	5	C-terminal	145
WHSPWSTP**PAPS**	13	4	N-terminal	31
LHWPLYTP**PASP**	12	4	N-terminal	33

[a] Residues contained in scoring window are shown in boldface type.
[b] Sum of pairwise comparisons of aligned residues within the scoring window.
[c] Position of first residue of the scoring window numbering from the N terminus of the mature protein.

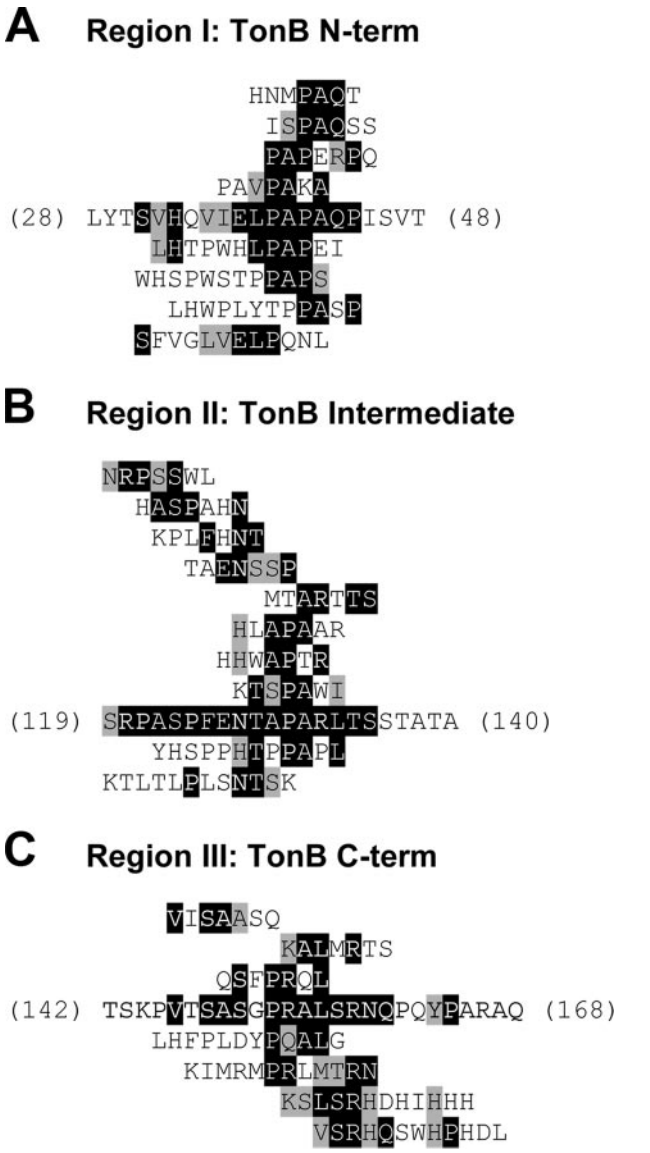

FIGURE 3. **Alignments of FhuD affinity-selected peptides to TonB.** *A*, region I, TonB N-terminal domain; *B*, region II, TonB intermediate domain; *C*, region III, TonB C-terminal domain. Peptides from the Ph.D.-12 library are aligned below the TonB sequence; peptides from the Ph.D.-C7C library are aligned above the TonB sequence. See Tables 3 and 4 for peptide match scores and window sizes. Alignment positions are highlighted according to their pairwise alignment score: +4, *black background* and *white characters*; +1, *gray background* and *dark characters*.

and the C-terminal domain (region III). Three-dimensional structural information has been reported (4, 5, 30) only for the C-terminal domain of TonB. We mapped (Fig. 4*A*) the cluster from region III to the NMR structure of the TonB C-terminal domain (PDB code 1XX3). Region III forms a continuous solvent-exposed binding surface on TonB (Fig. 4*B*), adjacent to FhuA-binding residues that we recently observed in the TonB-FhuA crystal structure (7). These observations suggest a potential FhuA-TonB-FhuD ternary complex. Because the three-dimensional structure of TonB residues in the N-terminal domain and intermediate domains are unknown, we consider the possibility that residues from TonB regions I and II could form a continuous FhuD-binding landscape with TonB region III.

Detection of a TonB-FhuD Complex by Dynamic Light Scattering—To identify and characterize a TonB-FhuD complex, we employed dynamic light scattering, a technique previously shown (31) to be effective for analyzing protein-protein complexes. Analysis of hydrodynamic distribution with the program Sedfit (25) revealed discrete hydrodynamic radii (Table 5) for all proteins, each with r.m.s.d. values less than 0.0097. Given its larger frictional ratio (20), TonB would exhibit a larger *Rh* despite a lower molecular mass compared with FhuD. Hence, TonB and FhuD exhibited similar *Rh* values. The *Rh* obtained from an equimolar mixture of these proteins indicated that a 1:1 heterocomplex had formed. As a control experiment, we observed an increase in *Rh* when a [Fhu switch-MBP] fusion protein harboring a previously characterized (24) TonB-binding peptide was mixed with TonB, indicating formation of a TonB-[Fhu switch-MBP] heterocomplex. No change in *Rh* was observed after mixing TonB with BSA, as compared with the *Rh* for each individual protein, indicating no formation of a TonB-BSA complex (data not shown).

To estimate the molecular mass of a TonB-FhuD heterocomplex, a DNS analysis was performed using Sedfit. Results from DNS analyses clearly indicated formation of a 1:1 TonB-FhuD heterocomplex. Molecular mass values for uncomplexed TonB

and uncomplexed FhuD determined by Sedfit from DLS autocorrelation data agree with their predicted values (Table 5, rows 1 and 2). A 1:1 mixture of TonB and FhuD resulted in formation of a scattering species with a refined molecular mass of 58 kDa (Table 5, row 3), corresponding to a 1:1 TonB-FhuD complex.

Both our phage display outcomes (24) and the x-ray crystallographic structure (7) of the TonB-FhuA complex demonstrated that residues in the switch helix region of FhuA interact directly with TonB. DLS analyses of [Fhu switch-MBP] fusion protein uncomplexed or in complex with TonB yielded results (Table 5, rows 4 and 5) in agreement with these previous analyses. The refined molecular mass for uncomplexed [Fhu switch-MBP] agreed with its predicted molecular mass. When [Fhu switch-MBP] was mixed with TonB in a 1:1 molar ratio, an abundant scattering species of ~61 kDa was observed, consistent with formation of a 1:1 heterocomplex between TonB and the fusion protein.

Detection of a TonB-FhuD Complex by Fluorescence Spectroscopy— Guided by the TonB-binding surface on FhuD that was predicted from phage display, we generated a mutant, FhuD T181C, to which were conjugated thiol-reactive probes capable of reporting changes in local environment. This mutant was assessed for its binding of ligand and for its binding of TonB. Rohrbach *et al.* (9) observed that addition of ferrichrome caused marked quenching of the intrinsic fluorescence of FhuD and used this observation to quantify binding of various ligands. We extended this feature to measure the ligand binding capacity of FhuD T181C. Addition of Fcn to either FhuD or to FhuD T181C caused substantial decreases in emission maxima. Binding curves were generated by plotting the percentage decrease in fluorescence as a function of Fcn added (Fig. 5*A*). Fits of these data (Table 6) to a single binding site model yielded similar apparent dissociation constants ($K_{D(app)}$) of either 1.2 ± 0.2 μM (FhuD) or 0.6 ± 0.2 μM (FhuD T181C), in agreement with the previously reported (9) K_D of 1 μM. Our results establish that the T181C mutation does not compromise ligand binding.

Taking advantage of the environmental sensitivity of the thiol-reactive probes AEDANS and MDCC, each probe was conjugated to FhuD T181C. Absorbance data (not shown) indicated that AEDANS labeled FhuD T181C at approximately a 1:1 ratio, consistent with Cys-181 being solvent-accessible and reactive. MDCC labeled ~1 mol of conjugate for every 3 mol of protein. This outcome likely resulted from labeling conditions. MDCC must be dissolved in Me_2SO; addition of this labeling solution to FhuD resulted in slight precipitation compared with the aqueous labeling conditions used with AEDANS, in which no precipitation was observed.

Upon addition of Fcn to AEDANS-labeled or to MDCC-labeled FhuD T181C, extrinsic fluorescence was quenched. Titration of these conjugates with Fcn is represented by the binding curves depicted in Fig. 5*B*. Fits of these data (Table 6) to a single binding site model yielded a similar $K_{D(app)}$ value as follows: 0.9 ± 0.2 μM for AEDANS-labeled FhuD T181C and 0.31 ± 0.03 μM for MDCC-labeled FhuD T181C. These binding constants agree with those determined by intrinsic protein fluorescence

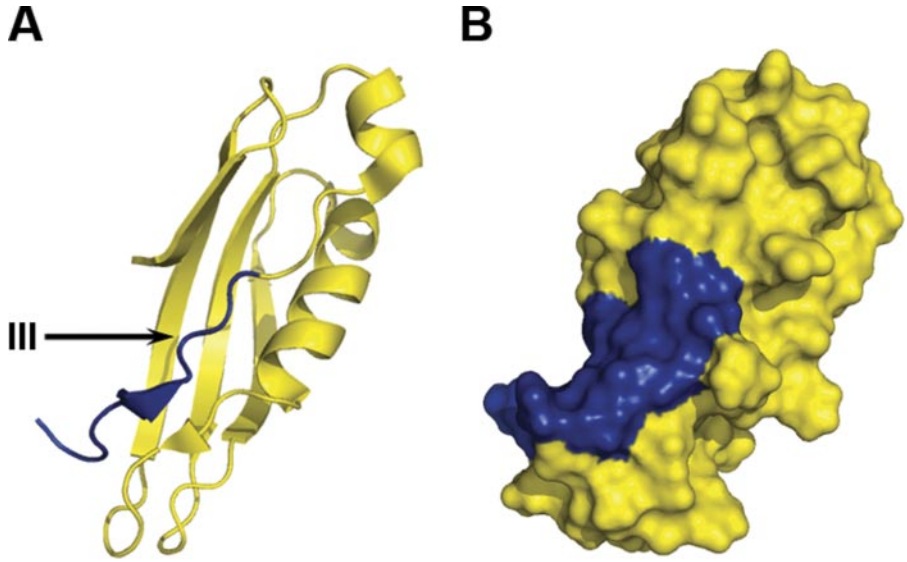

FIGURE 4. **FhuD-binding region identified by phage display mapped to TonB (PDB code 1XX3).** *A,* ribbon representation of the TonB C-terminal domain (*yellow*) with predicted FhuD-binding region III shaded *blue*. The region corresponding to RELIC/MATCH alignment cluster shown in Fig. 3*C* is indicated by the roman numeral *III*. *B,* molecular surface representation of TonB (*yellow*) with the predicted FhuD-binding region III shaded *blue*.

TABLE 5
DLS analysis of TonB, FhuD, and MBP-switch fusion

Protein	Hydrodynamic radius		Discrete non-interacting species			
			Molecular mass			
	Rh[a]	r.m.s.d.[b]	Predicted	Observed	Mass[c]	r.m.s.d.[d]
	nm		*Da*		%	
TonB	4.169	0.00707	25,065	26,482	67.4	0.00566
FhuD	4.188	0.00488	32,367	28,605	23.9	0.00470
TonB:FhuD (1:1)	5.023	0.00757	57,432	58,524	35.6	0.00584
[Fhu switch-MBP]	4.217	0.00669	41,970	39,526	53.8	0.00189
[Fhu switch-MBP]:TonB (1:1)	5.36	0.00963	67,035	60,993	44.8	0.00201

[a] *Rh*, hydrodynamic radius calculated from continuous intensity distribution model in Sedfit version 9.3.
[b] r.m.s.d., root mean square deviation from best fits to the autocorrelation curve for *Rh* analyses.
[c] Percent mass from DNS analyses, molecular mass >1000 kDa accounted for less than 11%, and the remainder was comprised of molecular mass <1.2 kDa.
[d] r.m.s.d. for discrete noninteracting species analysis.

and thus validate the utility of our experimental approach. Addition of Fcn quenched AEDANS and MDCC fluorescence, and this outcome reported on the occupancy of the FhuD siderophore-binding site.

FhuD T181C labeled with either AEDANS or MDCC demonstrated marked changes in fluorescence when mixed with TonB. Upon addition of TonB to labeled conjugates, quenching was observed (Fig. 6), demonstrating that the presence of TonB altered the environment of the probe. These changes were not observed when labeled FhuD T181C was mixed with an excess of BSA (data not shown). At low micromolar amounts of added TonB, saturation was achieved. Fits of these data to a single binding site model generated values as listed in Table 6. The $K_{D(app)}$ value for the TonB-FhuD complex was 0.31 ± 0.05 μM for AEDANS-labeled FhuD T181C and 0.27 ± 0.04 μM for MDCC-labeled FhuD T181C. Prior saturation of the FhuD-binding site with Fcn did not affect binding of TonB (Fig. 6) because similar dissociation constants (Table 6) were determined despite occupancy.

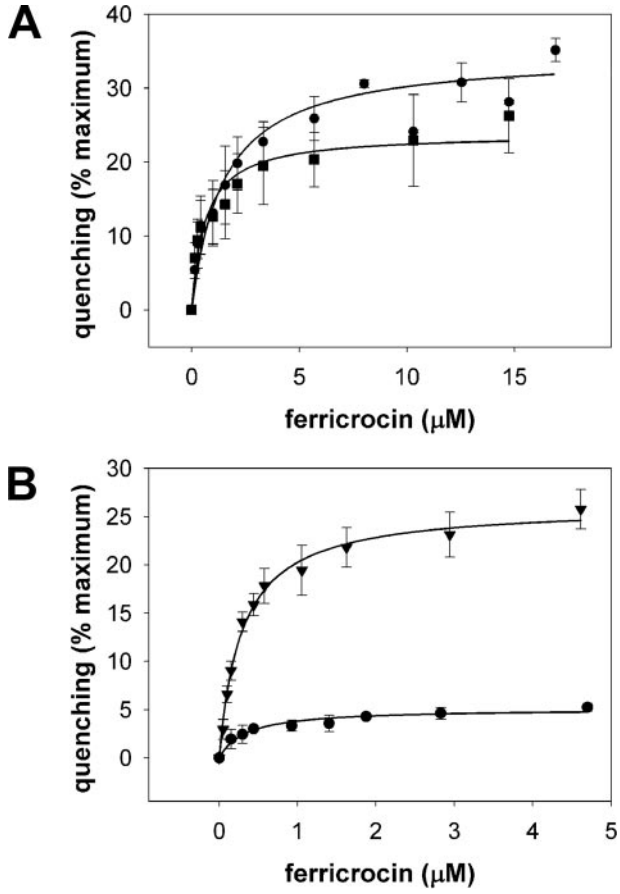

FIGURE 5. **Binding of Fcn to FhuD and to FhuD T181C.** *A*, FhuD (●) and FhuD T181C (■) were titrated with the indicated amounts of Fcn; quenching of intrinsic fluorescence is plotted as a function of Fcn concentration. *B*, binding of Fcn to AEDANS-labeled FhuD T181C (●) and to MDCC-labeled FhuD T181C (▼). Proteins were titrated with Fcn, and quenching of probe fluorescence was plotted as a function of Fcn added. *Error bars* in *A* and *B* represent the standard deviation from three independent experiments. *Lines* through data indicate best fits to a single binding site model as determined with Sigmaplot.

Given the spatial separation of putative interaction surfaces on TonB and FhuD, we attempted fits of our fluorescence data to a model describing two independent binding sites. When the data from titration of AEDANS-labeled FhuD T181C with TonB were fit to this model, a larger standard error was obtained, and the resulting $K_{D(app)}$ values were not meaningful (data not shown). Conversely, when the data from titration of MDCC-labeled FhuD T181C with TonB were fit to this model, the standard error improved compared with the single binding site model. However, the resulting $K_{D(app)}$ obtained from this procedure yielded large uncertainties confounding their interpretation. Although we cannot discount the possibility of two binding sites for TonB on FhuD, our results favor a single binding site.

Alteration of labeling conditions affected conjugation efficiencies. By labeling FhuD T181C overnight with AEDANS at 4 °C, 2 mol of label incorporated for every mol of protein. FhuD contains a single endogenous Cys-237. Based upon the x-ray crystal structure, this residue is not expected to be solvent-exposed. To determine whether Cys-237 was reactive to conjugation, we labeled FhuD by using the conditions above; unexpectedly, FhuD was labeled. Cys-237 localizes outside the phage display-identified TonB-binding surfaces. Given the reactivity of Cys-237 toward conjugation, we used this conjugate to exclude the possibility that TonB binds to regions other than those implicated by phage display. Addition of TonB to FhuD-AEDANS caused an insignificant increase in the fluorescence emission of AEDANS (data not shown). Given this outcome that contrasts with FhuD T181C-AEDANS, we consider that Cys-237 is not part of a TonB-binding environment. Our conclusion is that TonB binding localizes to regions on FhuD that were identified by phage display.

Detection of a TonB-FhuD Complex by Surface Plasmon Resonance—Our previous use of SPR technology quantified binding of FhuA to immobilized TonB (20). Given the outcomes of this experimental design, we adapted its use for the study of TonB-FhuD interactions. Dose-dependent binding of

TABLE 6

Summary of ligand binding parameters fit to a single site saturation ligand binding model

Data are from the following equation: $y = B_{max} \times [L]/(K_D + [L])$, where [L] indicates ligand concentration; reported uncertainties represent standard errors associated with best fits to the single binding site model.

FhuD	Titration with ferricrocin			Titration with TonB		
	Maximum quench	$K_{D(app)}$	R^2	Maximum quench	$K_{D(app)}$	R^2
	%	μM		%	μM	
Wild type	33 ± 2	1.2 ± 0.2	0.8857			
T181C	24 ± 2	0.6 ± 0.2	0.7725			
T181C-AEDANS	6.9 ± 0.4	0.9 ± 0.2	0.8368	5.8 ± 0.2	0.31 ± 0.05	0.9531
T181C-AEDANS + Fcn[a]				5.9 ± 0.3	0.4 ± 0.1	0.9323
T181C-MDCC	27 ± 1	0.31 ± 0.03	0.9614	70 ± 3	0.27 ± 0.04	0.9498
T181C-MDCC + Fcn				49 ± 3	0.5 ± 0.1	0.9765

[a] Fcn is ferricrocin.

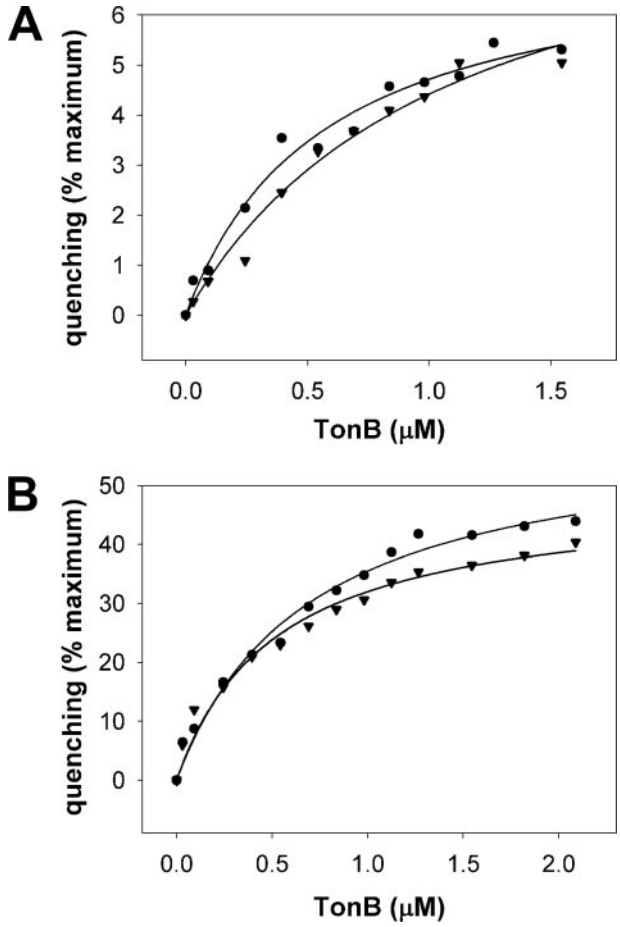

FIGURE 6. **Binding of TonB to AEDANS-labeled FhuD T181C and to MDCC-labeled FhuD T181C.** TonB was added to a solution of labeled FhuD (in the absence or presence of Fcn), and changes in extrinsic fluorescence were recorded. *A*, response upon addition of TonB to either FhuD T181C-AEDANS (●) or Fcn-bound FhuD T181C-AEDANS (▼). *B*, response upon addition of TonB to either FhuD T181C-MDCC (●) or Fcn-bound FhuD T181C-MDCC (▼). *Lines* through data indicate best fits to a single binding site model as determined with Sigmaplot. Results are representative of three experiments.

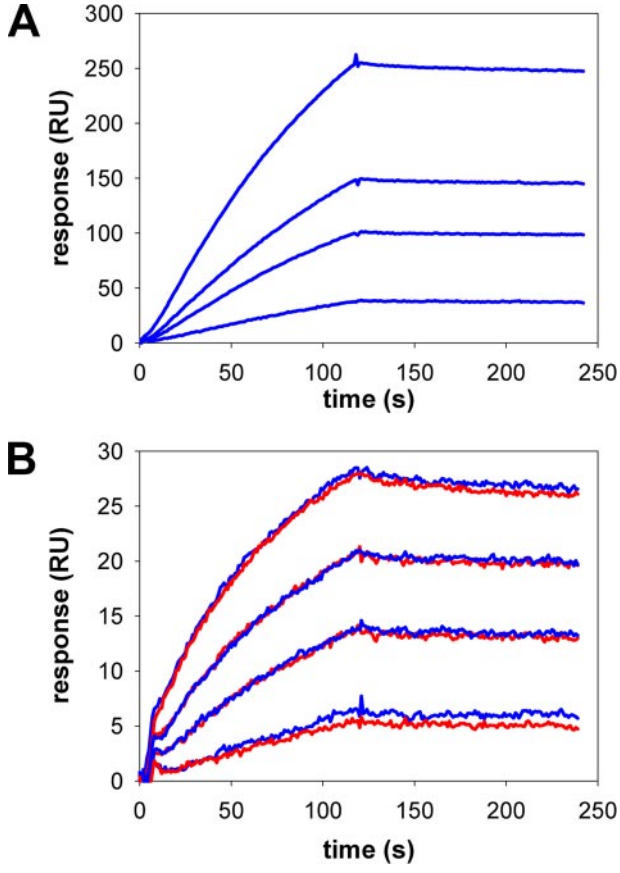

FIGURE 7. **Real time kinetics of TonB-FhuD binding interaction detected by SPR.** *A*, representative SPR sensogram for FhuD (*top to bottom*: 1000, 500, 250, and 100 nM) binding to amine-coupled TonB (250 RU) in the absence of Fcn. *B*, representative SPR sensogram for FhuD (*top to bottom*: 1000, 500, 250, and 100 nM) binding to thiol-coupled Cys-TonB (48 RU) in the absence (*blue*) or presence (*red*) of a 10-fold molar excess of Fcn.

FhuD to amine- and thiol-coupled TonB surfaces was observed (Fig. 7). Purified FhuA (0.1–1 μM) also bound to immobilized TonB as a positive control; FhuD binding (0.5 μM) was unaltered in the presence of BSA (0.5 μM) as a competitor (data not shown). To improve kinetic analyses, a homogeneous presentation of a lower density thiol-coupled Cys-TonB surface was utilized. A high affinity interaction (K_D ~20 nM) between FhuD and TonB was determined by SPR using a single binding site model. This interaction was characterized by slow association (k_a, ~2×10^4 M^{-1} s^{-1}) and slow dissociation rates (k_d, ~4×10^{-4} s^{-1}). Presence of the siderophore Fcn did not significantly alter the affinity between FhuD and TonB by SPR (Fig. 7*B*).

For reasons analogous to those considered with fluorescence data, we attempted to fit our SPR data to a model describing multiple binding sites. SPR data were fit to the heterogeneous ligand model, a model previously used to distinguish independent binding sites on biological macromolecules (32, 33). Similar to fluorescence, fits of the data to this model quantified two binding sites as follows: a high affinity site with K_D values in the low nanomolar range and a weak affinity site with K_D values in the low micromolar range. However, uncertainties associated with these fits confounded their interpretation. Because of this outcome, we favor a single site of interaction between TonB and FhuD.

By having established formation of a TonB-FhuD complex, we performed multicomponent SPR analyses to identify a ternary FhuA-TonB-FhuD complex. Initially, either a TonB-FhuA complex or a TonB-FhuD complex was formed by injecting each analyte over amine-coupled TonB surfaces. Once these binary complexes had formed, the secondary analyte was then injected. Injection of FhuD over a preformed TonB-FhuA complex indicated formation of a ternary FhuA-TonB-FhuD complex (Fig. 8*A*). Similarly, injection of FhuA over a previously formed TonB-FhuD complex indicated formation of a ternary FhuA-TonB-FhuD complex (Fig. 8*B*). Ternary complexes formed independent of the order of analyte addition. Qualitatively, association and dissociation rates were also independent of the order of analyte addition and mirrored those rates observed upon formation of each respective binary complex.

DISCUSSION

Translocation of siderophores into the cytoplasm of Gram-negative bacteria is partially understood, mainly with respect to the interplay between TonB and TonB-dependent OM receptors. However, molecular events occurring after translocation of siderophore into the periplasm remain largely unknown. Binding of the translocated iron-bound siderophore to the

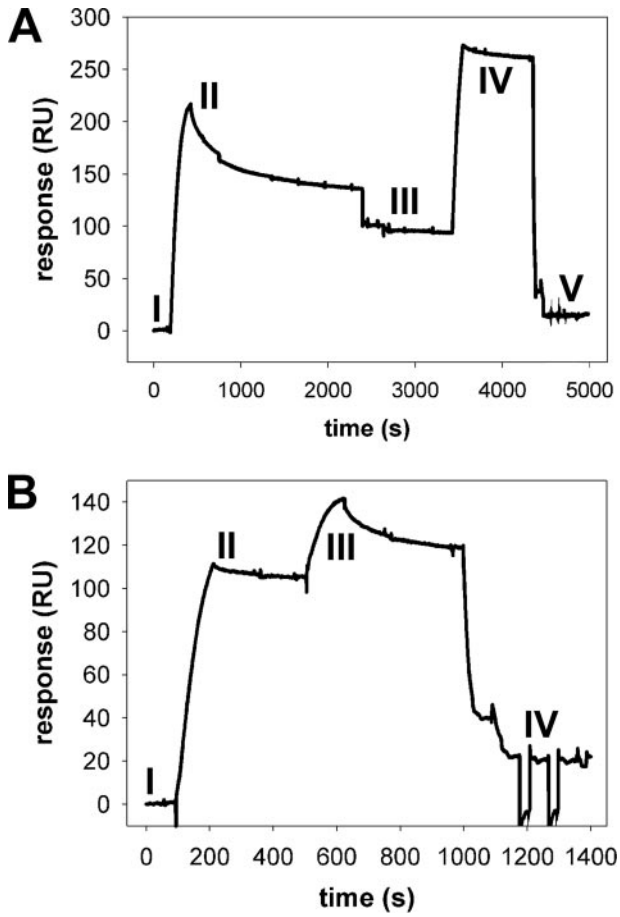

FIGURE 8. **Multicomponent SPR analysis to detect ternary complex formation between FhuA-TonB-FhuD.** *A,* SPR sensogram indicating the following: *I,* base line for buffer flowing over amine-coupled TonB (250 RU); *II,* increased signal change due to binding of FhuA (1 μM); *III,* stable FhuA-TonB complex after a 0.5 M NaCl wash; *IV,* increased signal change due to binding of FhuD (1 μM); *V,* return to base line after regeneration. *B,* SPR sensogram indicating the following: *I,* base line for buffer flowing over amine-coupled TonB (250 RU); *II,* increased signal change due to binding of FhuD (1 μM); *III,* increased signal change due to binding of FhuA (1 μM); *IV,* return to base line after regeneration.

periplasmic binding protein may be determined purely by diffusion within the periplasm. However, this mechanism poorly accounts for the weak affinity exhibited by FhuD toward its ligands. Sprencel *et al.* (34) determined a value of ~4,000 copies of the ferric enterobactin periplasmic binding protein FepB in *E. coli*, a low value compared with other periplasmic binding proteins such as those involved in sugar or amino acid transport. Köster and Braun (8) demonstrated that chromosomally encoded FhuD was undetectable from silver-stained SDS-polyacrylamide gels of periplasmic extracts. Taken together with the modest K_D value of 1.0 μM (9), these data suggest that diffusion alone would be insufficient to account for unidirectional siderophore transport. In addition to siderophore capture, diffusion-governed docking of siderophore-bound FhuD to the CM permease may be an inefficient process.

This study highlights novel interactions in the periplasm that are involved in siderophore uptake by *E. coli*. By exploiting phage display and adopting three biophysical strategies, we identified and mapped an interface between two interacting protein partners. On FhuD, a TonB-binding surface was identified that partially overlaps the FhuD siderophore-binding site. On TonB, three distinct regions of FhuD-binding surfaces were identified, two of which localized to regions for which no structural data exist. Given the apparent concordance between phage display (24) and structural biology (7), the regions identified in this study imply specific interactions between TonB and FhuD.

Interactions between TonB and FhuD are multidimensional. By DLS, we identified a 1:1 TonB-FhuD complex. Fluorescence spectroscopy indicated an apparent affinity for this complex to lie within the mid-nanomolar range. This affinity contrasts with the low nanomolar range determined by SPR. Our current SPR studies for FhuD-TonB are similar to the previous experimental design used to monitor the TonB-FhuA kinetics in real time (20). The affinity range predicted for TonB-FhuD interactions by SPR (low nanomolar) is consistent with the previously reported range (35) of TonB-FhuA interactions also by SPR. The differences in reported affinities between fluorescence and SPR may be attributed to solution phase *versus* immobilized systems or to buffer requirements of the different technologies. Given these differences, our data indicate that the affinity between TonB and FhuD lies somewhere in the low to mid-nanomolar range.

Significantly, the presence of Fcn did not alter the affinity between TonB and FhuD; there was no evidence for competition. However, the TonB-binding surface on FhuD as identified by phage display both overlaps the siderophore-binding site and extends beyond it; competition would not be expected. Furthermore, there is no evidence to suggest large conformational changes in FhuD upon binding siderophore (19). In the siderophore-bound state, FhuD probably maintains a rigid backbone; this rigidity would not influence binding of TonB. One implication of these findings is that interactions between siderophore and FhuD are distinct from interactions between TonB and FhuD. It remains to be determined whether siderophore can still bind to FhuD when complexed with TonB or whether bound TonB prevents siderophore binding through occlusion of siderophore-binding site for FhuD.

A regulated mechanism of siderophore transport would involve coordination of protein-protein interactions that would facilitate direct transfer of siderophore among protein partners. For such a mechanism, siderophore transfer would follow a sequence of directed exchanges from OM receptor, to periplasmic binding protein, to CM permease. Directed transfer of this sort would require a scaffold whereby protein-protein interactions drive spatial and temporal localization of the periplasmic binding protein to regions involved in siderophore translocation activities. The dynamic nature by which TonB cycles or changes its conformation during energy transduction offers itself as an ideal candidate to fulfill this role.

Our SPR data indicated formation of a ternary FhuA-TonB-FhuD complex. This finding, taken together with the recent structural determinations of TonB bound to FhuA (7) and to BtuB (36), underscores the possibility of such a complex. It would position a periplasmic binding protein to accept siderophore immediately after its translocation through a TonB-dependent OM receptor. Examination of the TonB-FhuA interaction surface provides a means to evaluate residues involved in the protein-protein interaction. In the TonB-FhuA crystal structure, residues N-terminal to Arg-158 on TonB were

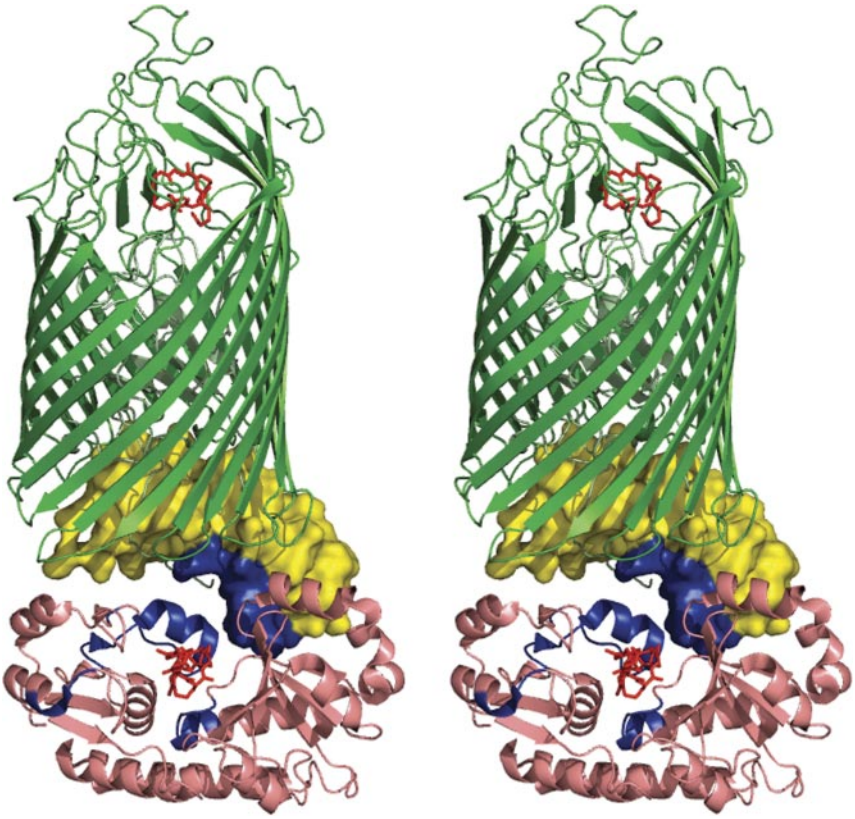

FIGURE 9. **Model of a FhuA-TonB-FhuD ternary complex.** Stereo image depicting a possible ternary complex between FhuA, TonB, and FhuD. FhuD (PDB code 1EFD) was manually docked under the TonB-FhuA crystal structure (PDB code 2GRX) using phage display-identified protein-protein interaction surfaces as docking constraints. Complementary phage display-identified surfaces are colored *blue* on both TonB (*yellow*, surface representation) and FhuD (*salmon*, ribbon representation). The orientation localizes the FhuD siderophore-binding site beneath the lumen of FhuA (*green*, ribbon representation). For clarity, a molecular surface is projected on TonB.

not resolved and may not participate in the TonB-FhuA interface. The FhuD-interacting residues on TonB that were predicted by phage display (Fig. 3*C, region III*) localize immediately N-terminal to TonB Arg-158. We infer that these residues are poised to bind FhuD in a FhuA-TonB-FhuD ternary complex.

Given these experimental outcomes, we propose a structural model for a FhuA-TonB-FhuD complex. Examination of complementary binding regions on solvent-accessible surfaces for known TonB and FhuD structures reveals no obvious means by which the two proteins can interact. However, one can rationally position FhuD to the TonB-FhuA structure using these surfaces as docking constraints. Fig. 9 depicts a model for a ternary FhuA-TonB-FhuD complex that is based on our experimental evidence. In this model, FhuD-binding regions on TonB are colored according to the convention adopted in Fig. 4. TonB residues ^{153}PRALS^{157} corresponding to region III (Fig. 3*C*) were computationally modeled at its N terminus. Their position illustrates that interaction with FhuD at this region would result in the apposition of its siderophore-binding site with the FhuA lumen such that it would intersect with the trajectory of the translocated siderophore. Furthermore, TonB residues interacting with FhuA in the TonB-FhuA crystal structure are distal to those TonB residues that contact FhuD. Separation of these binding surfaces may therefore coordinate transduction of energy to FhuA with directed localization of FhuD beneath the FhuA lumen.

The precise sequence of these events has yet to be established. Our data cannot distinguish whether FhuD remains bound to TonB during the energy transduction cycle or if binding is a transient event. One possibility is that FhuD binds and dissociates as a function of the TonB energy transduction cycle, perhaps resulting from the β-strand exchange that TonB is known to undergo (4, 5, 7, 30, 36). Prolonged association of FhuD with TonB seems unlikely as FhuD must ultimately deliver siderophore to FhuB/C. It is intriguing that the most extreme N-terminal FhuD-binding surface on TonB is at a region close to probable contact sites with ExbB/ExbD. Such placement may be a means by which TonB directs transfer of FhuD from the OM to CM as TonB disengages FhuA. This mechanism would ensure that FhuD samples a space proximal to the CM, thereby enhancing the probability of encountering FhuB. Previous reports have indicated (14, 37) that interactions between the FhuD homologue BtuF and its cognate transporter BtuC/D are virtually irreversible. This observation remains to be clarified in light of our experimental evidence, which for the first time identifies TonB as a binding partner for periplasmic binding proteins. We advocate a mechanism favoring transient associations of periplasmic siderophore-binding proteins with TonB and with their cognate CM transporters at discrete steps during the siderophore transport cycle.

We previously used phage display in concert with biophysical methods to map unambiguously the network of protein-protein interactions that occur at the TonB-FhuA interface. These outcomes were recently confirmed by the x-ray structure of the TonB-FhuA complex. This strategy is now extended to identify interfaces involved in TonB-FhuD interactions. Such interactions may serve to coordinate spatial and temporal localization of periplasmic binding proteins to environments involved in siderophore uptake. Given the diversity of components among different siderophore transport systems, we propose that in addition to its role as energy transducer, TonB acts as a unifying element, a scaffold to regulate the unidirectional flow of iron-bound siderophore from the OM to the CM.

Acknowledgments—The Canada Foundation for Innovation awarded infrastructure to the Montreal Integrated Genomics Group for Research on Infectious Pathogens. Sheldon Biotechnology Centre at McGill University is supported by multiuser maintenance grants from Canadian Institutes of Health Research. We appreciate the contributions of experimental materials by M. Damlaj, J. Deme, J. Gilbert, K. James, and C. Ng. We also thank J. A. Kashul for editorial support.

REFERENCES

1. Wandersman, C., and Delepelaire, P. (2004) *Annu. Rev. Microbiol.* **58,** 611–647
2. Ferguson, A. D., Hofmann, E., Coulton, J. W., Diederichs, K., and Welte, W. (1998) *Science* **282,** 2215–2220
3. Locher, K. P., Rees, B., Koebnik, R., Mitschler, A., Moulinier, L., Rosenbusch, J. P., and Moras, D. (1998) *Cell* **95,** 771–778
4. Chang, C., Mooser, A., Plückthun, A., and Wlodawer, A. (2001) *J. Biol. Chem.* **276,** 27535–27540
5. Ködding, J., Killig, F., Polzer, P., Howard, S. P., Diederichs, K., and Welte, W. (2005) *J. Biol. Chem.* **280,** 3022–3028
6. Peacock, R. S., Andrushchenko, V. V., Demcoe, A. R., Gehmlich, M., Lu, L. S., Herrero, A. G., and Vogel, H. J. (2006) *Biometals* **19,** 127–142
7. Pawelek, P. D., Croteau, N., Ng-Thow-Hing, C., Khursigara, C. M., Moiseeva, N., Allaire, M., and Coulton, J. W. (2006) *Science* **312,** 1399–1402
8. Köster, W., and Braun, V. (1990) *J. Biol. Chem.* **265,** 21407–21410
9. Rohrbach, M. R., Braun, V., and Köster, W. (1995) *J. Bacteriol.* **177,** 7186–7193
10. Mademidis, A., Killmann, H., Kraas, W., Flechsler, I., Jung, G., and Braun, V. (1997) *Mol. Microbiol.* **26,** 1109–1123
11. Schultz-Hauser, G., Köster, W., Schwarz, H., and Braun, V. (1992) *J. Bacteriol.* **174,** 2305–2311
12. Clarke, T. E., Ku, S. Y., Dougan, D. R., Vogel, H. J., and Tari, L. W. (2000) *Nat. Struct. Biol.* **7,** 287–291
13. Clarke, T. E., Braun, V., Winkelmann, G., Tari, L. W., and Vogel, H. J. (2002) *J. Biol. Chem.* **277,** 13966–13972
14. Borths, E. L., Locher, K. P., Lee, A. T., and Rees, D. C. (2002) *Proc. Natl. Acad. Sci. U. S. A.* **99,** 16642–16647
15. Karpowich, N. K., Huang, H. H., Smith, P. C., and Hunt, J. F. (2003) *J. Biol. Chem.* **278,** 8429–8434
16. Lee, Y. H., Deka, R. K., Norgard, M. V., Radolf, J. D., and Hasemann, C. A. (1999) *Nat. Struct. Biol.* **6,** 628–633
17. Lawrence, M. C., Pilling, P. A., Epa, V. C., Berry, A. M., Ogunniyi, A. D., and Paton, J. C. (1998) *Structure* (*Lond.*) **6,** 1553–1561
18. Krewulak, K. D., Peacock, R. S., and Vogel, H. J. (2004) in *Iron Transport in Bacteria* (Crosa, J. H., Mey, A. R., and Payne, S. M., eds) pp. 113–129, American Society for Microbiology, Washington, D. C.
19. Krewulak, K. D., Shepherd, C. M., and Vogel, H. J. (2005) *Biometals* **18,** 375–386
20. Khursigara, C. M., De Crescenzo, G., Pawelek, P. D., and Coulton, J. W. (2004) *J. Biol. Chem.* **279,** 7405–7412
21. Khursigara, C. M., De Crescenzo, G., Pawelek, P. D., and Coulton, J. W. (2005) *Biochemistry* **44,** 3441–3453
22. Moeck, G. S., and Letellier, L. (2001) *J. Bacteriol.* **183,** 2755–2764
23. Rohrbach, M. R., Paul, S., and Köster, W. (1995) *Mol. Gen. Genet.* **248,** 33–42
24. Carter, D. M., Gagnon, J. N., Damlaj, M., Mandava, S., Makowski, L., Rodi, D. J., Pawelek, P. D., and Coulton, J. W. (2006) *J. Mol. Biol.* **357,** 236–251
25. Schuck, P. (2000) *Biophys. J.* **78,** 1606–1619
26. Yang, Y. R., and Schachman, H. K. (1996) *Biophys. Chem.* **59,** 289–297
27. Lebowitz, J., Lewis, M. S., and Schuck, P. (2002) *Protein Sci.* **11,** 2067–2079
28. Myszka, D. G. (1999) *J. Mol. Recognit.* **12,** 279–284
29. Mandava, S., Makowski, L., Devarapalli, S., Uzubell, J., and Rodi, D. J. (2004) *Proteomics* **4,** 1439–1460
30. Peacock, R. S., Weljie, A. M., Howard, S. P., Price, F. D., and Vogel, H. J. (2005) *J. Mol. Biol.* **345,** 1185–1197
31. Lamb, A. L., Torres, A. S., O'Halloran, T. V., and Rosenzweig, A. C. (2000) *Biochemistry* **39,** 14720–14727
32. Mader, C., Huber, C., Moll, D., Sleytr, U. B., and Sára, M. (2004) *J. Bacteriol.* **186,** 1758–1768
33. Nakajima, H., Cocquerel, L., Kiyokawa, N., Fujimoto, J., and Levy, S. (2005) *Biochem. Biophys. Res. Commun.* **328,** 1091–1100
34. Sprencel, C., Cao, Z., Qi, Z., Scott, D. C., Montague, M. A., Ivanoff, N., Xu, J., Raymond, K. M., Newton, S. M., and Klebba, P. E. (2000) *J. Bacteriol.* **182,** 5359–5364
35. Khursigara, C. M., De Crescenzo, G., Pawelek, P. D., and Coulton, J. W. (2005) *Protein Sci.* **14,** 1266–1273
36. Shultis, D. D., Purdy, M. D., Banchs, C. N., and Wiener, M. C. (2006) *Science* **312,** 1396–1399
37. Borths, E. L., Poolman, B., Hvorup, R. N., Locher, K. P., and Rees, D. C. (2005) *Biochemistry* **44,** 16301–16309

Interactions between TonB from *Escherichia coli* and the Periplasmic Protein FhuD

David M. Carter, Isabelle R. Miousse, Jean-Nicolas Gagnon, Éric Martinez, Abigail Clements, Jongchan Lee, Mark A. Hancock, Hubert Gagnon, Peter D. Pawelek and James W. Coulton

J. Biol. Chem. 2006, 281:35413-35424.
doi: 10.1074/jbc.M607611200 originally published online August 23, 2006
